



Novikov, Sergei V. and Staddon, Christopher R. and Sahonta, S-L and Oliver, R.A. and Humphreys, C.J. and Foxon, C.T. (2016) Growth of free-standing bulk wurtzite  $\text{Al}_x\text{Ga}_{1-x}\text{N}$  layers by molecular beam epitaxy using a highly efficient RF plasma source. *Journal of Crystal Growth* . ISSN 0022-0248

**Access from the University of Nottingham repository:**

<http://eprints.nottingham.ac.uk/35729/1/1-s2.0-S0022024816303931-main.pdf>

**Copyright and reuse:**

The Nottingham ePrints service makes this work by researchers of the University of Nottingham available open access under the following conditions.

This article is made available under the Creative Commons Attribution licence and may be reused according to the conditions of the licence. For more details see: <http://creativecommons.org/licenses/by/2.5/>

**A note on versions:**

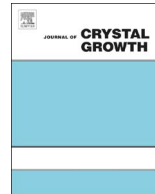
The version presented here may differ from the published version or from the version of record. If you wish to cite this item you are advised to consult the publisher's version. Please see the repository url above for details on accessing the published version and note that access may require a subscription.

For more information, please contact [eprints@nottingham.ac.uk](mailto:eprints@nottingham.ac.uk)



Contents lists available at ScienceDirect

## Journal of Crystal Growth

journal homepage: [www.elsevier.com/locate/jcrysgr](http://www.elsevier.com/locate/jcrysgr)

# Growth of free-standing bulk wurtzite $\text{Al}_x\text{Ga}_{1-x}\text{N}$ layers by molecular beam epitaxy using a highly efficient RF plasma source

S.V. Novikov<sup>a,\*</sup>, C.R. Staddon<sup>a</sup>, S.-L. Sahonta<sup>b</sup>, R.A. Oliver<sup>b</sup>, C.J. Humphreys<sup>b</sup>, C.T. Foxon<sup>a</sup>

<sup>a</sup> School of Physics and Astronomy, University of Nottingham, Nottingham NG7 2RD, UK

<sup>b</sup> Department of Materials Science and Metallurgy, University of Cambridge, Cambridge CB3 0FS, UK

## ARTICLE INFO

## Keywords:

- A1. Substrates
- A3. Molecular beam epitaxy
- B1. Nitrides
- B2. Semiconducting III–V materials

## ABSTRACT

The recent development of group III nitrides allows researchers world-wide to consider AlGa<sub>x</sub>N based light emitting diodes as a possible new alternative deep ultra-violet light source for surface decontamination and water purification. In this paper we will describe our recent results on plasma-assisted molecular beam epitaxy (PA-MBE) growth of free-standing wurtzite  $\text{Al}_x\text{Ga}_{1-x}\text{N}$  bulk crystals using the latest model of Riber's highly efficient nitrogen RF plasma source. We have achieved AlGa<sub>x</sub>N growth rates up to 3 μm/h. Wurtzite  $\text{Al}_x\text{Ga}_{1-x}\text{N}$  layers with thicknesses up to 100 μm were successfully grown by PA-MBE on 2-inch and 3-inch GaAs (111)B substrates. After growth the GaAs was subsequently removed using a chemical etch to achieve free-standing  $\text{Al}_x\text{Ga}_{1-x}\text{N}$  wafers. Free-standing bulk  $\text{Al}_x\text{Ga}_{1-x}\text{N}$  wafers with thicknesses in the range 30–100 μm may be used as substrates for further growth of  $\text{Al}_x\text{Ga}_{1-x}\text{N}$ -based structures and devices. High Resolution Scanning Transmission Electron Microscopy (HR-STEM) and Convergent Beam Electron Diffraction (CBED) were employed for detailed structural analysis of AlGa<sub>x</sub>N/GaAs (111)B interface and allowed us to determine the N-polarity of AlGa<sub>x</sub>N layers grown on GaAs (111)B substrates. The novel, high efficiency RF plasma source allowed us to achieve free-standing  $\text{Al}_x\text{Ga}_{1-x}\text{N}$  layers in a single day's growth, making this a commercially viable process.

© 2016 The Authors. Published by Elsevier B.V. This is an open access article under the CC BY license (<http://creativecommons.org/licenses/by/4.0/>).

## 1. Introduction

The recent development of group III nitrides allows researchers world-wide to consider AlGa<sub>x</sub>N based light emitting diodes (LEDs) as a possible new alternative deep ultra-violet (DUV) light source for surface decontamination and water purification [1–5]. If efficient devices can be developed they will be easy to use, have potentially a long life time, be mechanically robust and will lend themselves to battery operation to allow their use in remote locations. Changing the composition of the active AlGa<sub>x</sub>N layer, will allow one to tune easily the wavelength of the LEDs. This has stimulated active research world-wide to develop AlGa<sub>x</sub>N based LEDs [2–5]. Such DUV LEDs will also have potential applications for solid state lighting and drug detection.

The first successful semiconductor UV LEDs are now manufactured using the  $\text{Al}_x\text{Ga}_{1-x}\text{N}$  material system, covering the energy range from 3.4 up to 6.2 eV. One of the most severe problems hindering the progress of DUV LEDs is the lack of suitable substrates on which lattice-matched AlGa<sub>x</sub>N films can be grown [1–5]. Currently the majority of AlGa<sub>x</sub>N DUV LED devices are grown on

sapphire or AlN. The consequence of a poor lattice match is a very high defect density in the films, which can impair device performance. The lattice mismatch between the substrate (sapphire or AlN) and the active AlGa<sub>x</sub>N layer results in poor structural quality of the layers, cracks, and low radiative recombination rates in current DUV LED devices. As a result, AlGa<sub>x</sub>N layers contain a high density of dislocations arising from the large lattice mismatch and the difference in thermal expansion coefficient between the AlGa<sub>x</sub>N layers and sapphire, which results in a low ~1–10% external quantum efficiency (EQE) and poor reliability of existing DUV LEDs. DUV LEDs require an AlN content in the mid-range between pure AlN and GaN, and therefore high quality ternary AlGa<sub>x</sub>N substrates may significantly improve the properties of the devices. However, only limited success has been achieved so far in the growth of bulk  $\text{Al}_x\text{Ga}_{1-x}\text{N}$  crystals with a variable AlN content [6,7].

Molecular beam epitaxy (MBE) is normally regarded as an epitaxial technique for the growth of very thin layers with monolayer control of their thickness. However, we have used the plasma-assisted molecular beam epitaxy (PA-MBE) technique for bulk crystal growth and have produced free-standing layers of wurtzite  $\text{Al}_x\text{Ga}_{1-x}\text{N}$  wafers [8]. Thick wurtzite  $\text{Al}_x\text{Ga}_{1-x}\text{N}$  films with an AlN content from 0 to 0.5 were successfully grown by PA-MBE on 2-inch GaAs (111)B substrates. However, in our previous

\* Corresponding author.

E-mail address: [Sergei.Novikov@Nottingham.ac.uk](mailto:Sergei.Novikov@Nottingham.ac.uk) (S.V. Novikov).

studies the growth rate for  $\text{Al}_x\text{Ga}_{1-x}\text{N}$  films remained below  $1 \mu\text{m/h}$  and this is too slow to make the process commercially viable.

Recent years have seen significant effort from the main MBE manufacturers in France, USA and Japan to increase the efficiency of their nitrogen RF plasma sources to allow higher growth rates for GaN-based alloys. All of the manufacturers are exploring the route of increasing the conductance of the aperture plates of the RF plasma cavity in order to achieve significantly higher total flows of nitrogen through the plasma source. For example, in the recent Riber source the conductance of the aperture plate has been increased by increasing the number of 0.3 mm diameter holes to 1200 [9]. With this Riber source we have achieved growth rates for thick GaN layers of up to  $1.8 \mu\text{m/h}$  on 2-inch diameter GaAs (111)B and sapphire wafers [10].

Recently, Riber have again modified the design of the aperture plate of their plasma source for even faster growth of GaN layers. The aperture conductance has been increased significantly by an increase in the number of holes, which allows a further increase in the GaN growth rate. First tests of the latest model of Riber RF nitrogen plasma source with 5880 holes in the aperture plate, produced even higher growth rates for thin GaN layers up to  $7.6 \mu\text{m/h}$ , but with nitrogen flow rates of about 25 sccm [11].

In this paper we will describe our recent results on PA-MBE growth of free-standing wurtzite  $\text{Al}_x\text{Ga}_{1-x}\text{N}$  bulk crystals on up to 3-inch diameter substrates using the latest Riber model of the highly efficient nitrogen RF plasma source. Special emphasis in the current study has been made on the detailed structural analysis of AlGaN/GaAs (111)B interface.

## 2. Experimental details

Wurtzite GaN and  $\text{Al}_x\text{Ga}_{1-x}\text{N}$  films were grown by PA-MBE in a MOD-GENII system [8]. 2-inch and 3-inch diameter sapphire and GaAs (111)B were used as substrates. The active nitrogen for the growth of the group III-nitrides was provided by a novel high efficiency plasma source from Riber RF-N 50/63 with 5880 holes in the aperture plate. The source was custom designed at Riber in order to match the dimensions of MOD-GENII Varian system source flanges. The use of an  $\text{As}_2$  flux of  $\sim 6 \times 10^{-6}$  Torr beam equivalent pressure (BEP) during substrate heating and the removal of the surface oxide from the GaAs (111)B substrates allowed us to avoid any degradation of the GaAs substrate surface. The arsenic flux was terminated at the start of the GaN growth. A thin GaN buffer was deposited before the growth of the  $\text{Al}_x\text{Ga}_{1-x}\text{N}$  layers. In the current study, the  $\text{Al}_x\text{Ga}_{1-x}\text{N}$  layers were grown at temperatures of  $\sim 700^\circ\text{C}$ . We are not able to use higher growth temperatures due to the low thermal stability of the GaAs substrates in vacuum above  $700^\circ\text{C}$ , even under an  $\text{As}_2$  flux.

The  $\text{Al}_x\text{Ga}_{1-x}\text{N}$  layers with thicknesses up to  $100 \mu\text{m}$  were grown on GaAs substrates, and the GaAs was subsequently removed using a chemical etch to achieve free-standing  $\text{Al}_x\text{Ga}_{1-x}\text{N}$  wafers. From our previous experience with MBE growth of bulk zinc-blende and wurtzite  $\text{Al}_x\text{Ga}_{1-x}\text{N}$  [8], such thicknesses are already sufficient to obtain free-standing  $\text{Al}_x\text{Ga}_{1-x}\text{N}$  layers.

The structural properties of the samples were studied *in-situ* using reflection high-energy electron diffraction (RHEED) and after growth *ex-situ* measurements were performed using X-ray diffraction (XRD) and Transmission Electron Microscopy (TEM). A Philips X'Pert MRD diffractometer was used for XRD analysis of the layers. Advanced TEM studies were performed using an FEI Titan microscope operating at 300 kV with a CEOS probe-side corrector, and a JEOL 4000 EX microscope operating at 400 kV. Specimens were prepared for TEM by mechanical polishing, dimple grinding and ion milling with an argon ion beam at an acceleration voltage of 4 kV.

We have studied the uniformity of Al incorporation in the  $\text{Al}_x\text{Ga}_{1-x}\text{N}$  layers by secondary ion mass spectrometry (SIMS) using Cameca IMS-3F and IMS-4F systems and using an Oxford Instruments EDX system.

## 3. Results and discussion

The best structural properties of free-standing wurtzite AlGaN layers can be achieved with initiation under Ga-rich conditions, but before the formation of Ga droplets [8]. Therefore, the first step for us with the use of the novel RF plasma source is to establish optimum growth conditions for a given nitrogen flux. In the current study we used a nitrogen flow rate of 6 sccm; which allowed us to use our standard PA-MBE pumping configuration for the MOD-GENII system with a CT-8 cryopump. We have grown GaN layers on 2" sapphire wafers to simplify the initiation process. In the case of GaAs substrates one need to be very precise at the GaN initiation stages to prevent potential strong meltback etching of the GaAs wafers, The beam equivalent pressure (BEP) of nitrogen in the chamber during growth did not exceed  $2 \times 10^{-4}$  Torr. All layers were grown with a fixed RF power of 500 W. We achieved a growth rate of  $3 \mu\text{m/h}$  at a Ga flux of  $\sim 2 \times 10^{-6}$  Torr. At the higher Ga fluxes the growth rate remains the same and we observed the formation of Ga droplets on the GaN surface under strongly Ga-rich conditions.

We have used slightly Ga-rich conditions, but before the formation of Ga droplets for the growth of thick wurtzite  $\text{Al}_x\text{Ga}_{1-x}\text{N}$  layers on (111)B GaAs substrates. We have shown previously that growth on (111)B orientation allows us to initiate the growth of hexagonal phase material [8]. Wurtzite GaN buffers, 50–200 nm thick, were deposited before the growth of the  $\text{Al}_x\text{Ga}_{1-x}\text{N}$  layers.

In MBE, the substrate temperature is normally measured using an optical pyrometer. In the case of transparent sapphire substrates, the pyrometer measures the temperature of the substrate heater, not the substrate surface. Our estimate of the growth temperature on sapphire was based on a thermocouple reading. In the case of GaAs wafers we can measure and control the growth temperature with pyrometer. Therefore, we may have slightly different growth temperatures on sapphire and on (111)B GaAs wafers.

High-resolution TEM studies were used to investigate the interface between the GaAs substrate and GaN layer as shown in Fig. 1. We observed zinc-blende GaN crystallites in the wurtzite GaN matrix close to the GaAs substrate interface. These cubic inclusions extend to the first few tens of nanometers (less than 100 nm) into the GaN wurtzite film, before being terminated at (0001) basal plane stacking faults, which form boundaries with

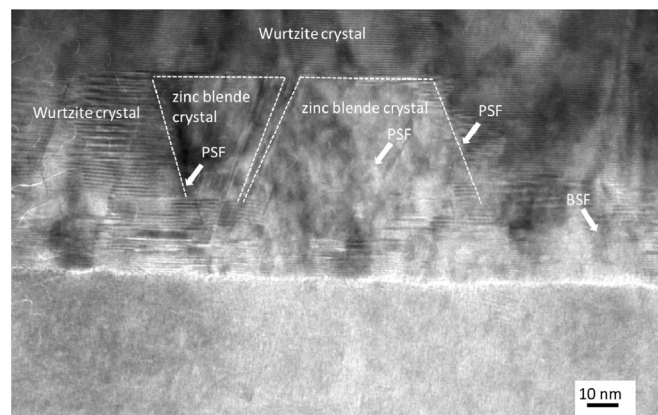


Fig. 1. High-resolution TEM image of a GaN/GaAs (111) B substrate interface.

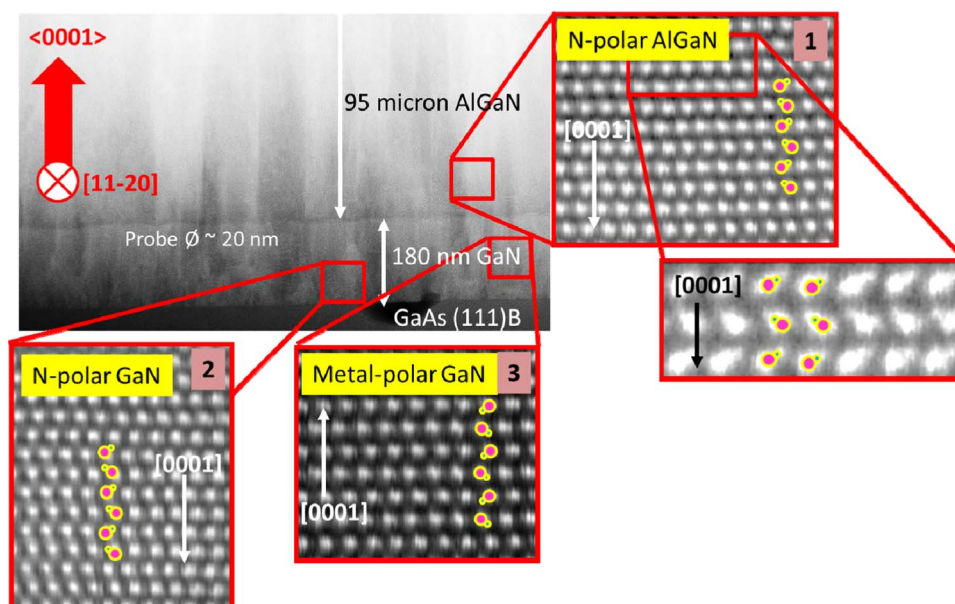


Fig. 2. HR-STEM image of the AlGaN/GaN/GaAs (111)B substrate interface.

the wurtzite matrix. We also see the roughening of the surface of the GaAs due to plasma- or melt-back etching of the substrate. Arsenic contamination of the first few nanometers of the layer is possibly responsible for the formation of the zinc-blende grains.

From general considerations one might expect that GaN layers grown on a GaAs (111)A surface will exhibit Ga-polarity, but N-polarity will become preferable for the growth on GaAs (111)B substrates. However, as has been shown previously this may depend strongly on the MBE growth conditions [12].

The polarity of our AlGaN and GaN layers grown with high growth rates on (111)B GaAs have been investigated using high resolution Scanning Transmission Electron Microscopy (HR-STEM). Fig. 2 shows HR-STEM images of three areas of the GaN buffer and AlGaN film viewed at atomic resolution. The AlGaN film clearly shows N-polarity due to the relative positions of the individual nitrogen atomic columns with respect to the gallium atom columns in the wurtzite crystal along the [0001] direction. The polarity of the AlGaN layer was verified by Convergent Beam Electron Diffraction (CBED) studies (not shown), which confirmed N-polarity in the AlGaN film. However there appear to be isolated regions of mixed polarity in the GaN buffer layer, as shown by two atomic resolution images of different GaN regions which suggest that both N- and Ga-polar regions occur. This may be due to isolated N-polar regions forming by growth on meltback-etched regions of the GaAs substrate, however no inversion domain boundaries were observed in the buffer region, so it is not known whether these mixed polarity regions occur in high densities. The high density of extended defects in the GaN buffer layer resulted in scattering effects in CBED patterns, preventing conclusive CBED information about GaN buffer film polarity to be measured.

Based on these results, we then grew thicker wurtzite  $\text{Al}_x\text{Ga}_{1-x}\text{N}$  layers under similar group III-rich growth conditions on (111)B GaAs substrates using the second generation Riber source. Fig. 3 demonstrates that the  $\text{Al}_x\text{Ga}_{1-x}\text{N}$  layer thickness increases linearly with growth time. We have observed the growth rate of  $\sim 2.2 \mu\text{m}/\text{h}$ , which is lower than we can see on sapphire wafers under similar conditions. This is probably result of different growth surface temperature or different Ga(Al) re-evaporation on sapphire and GaAs substrates, but this question is still under investigation.

Fig. 4 shows a  $2\theta$ - $\omega$  XRD plot for a  $\sim 105 \mu\text{m}$  thick wurtzite  $\text{Al}_x$

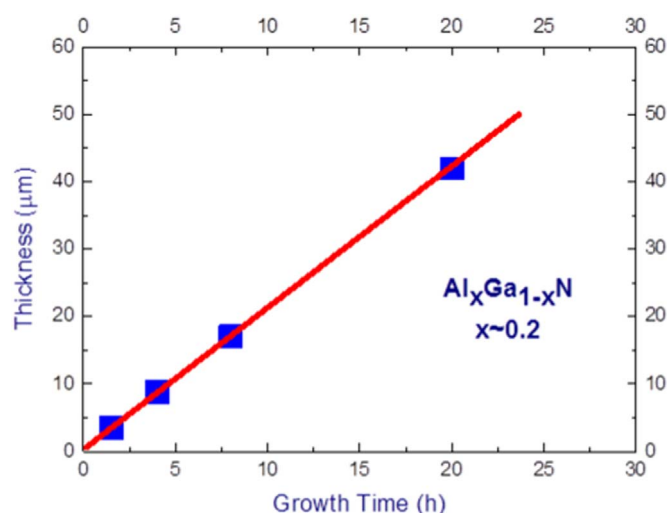


Fig. 3. Thickness dependence on the growth time for  $\text{Al}_x\text{Ga}_{1-x}\text{N}$  layers ( $x \sim 0.2$ ) on 2-inch sapphire (6 sccm  $\text{N}_2$  flow at 500 W).

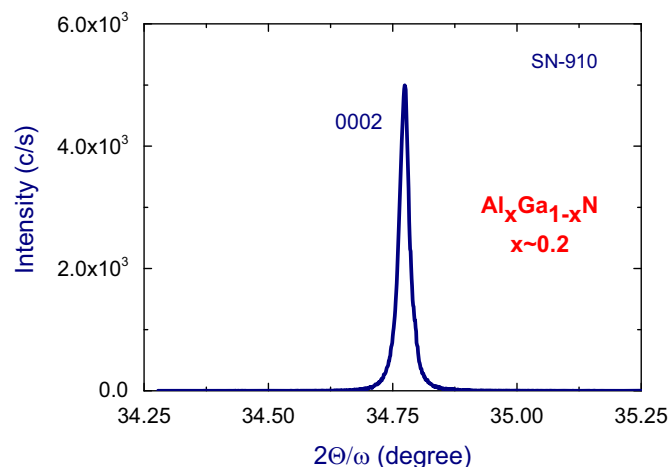


Fig. 4.  $2\theta$ - $\omega$  XRD scan of the 0002 peak for a wurtzite  $\text{Al}_x\text{Ga}_{1-x}\text{N}$  layer ( $x \sim 0.2$ ; thickness  $\sim 105 \mu\text{m}$ ).



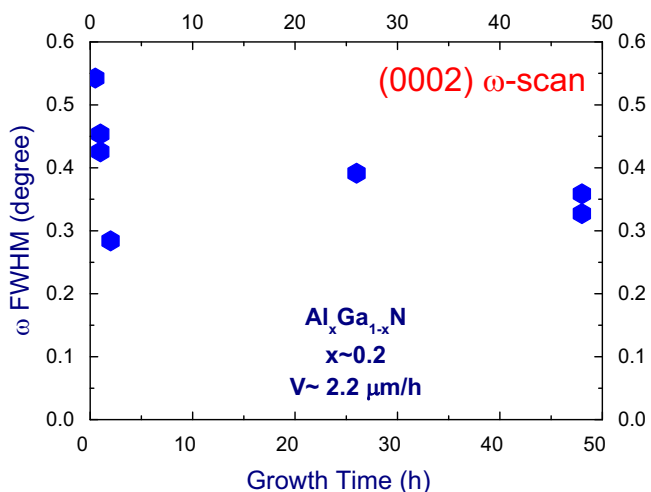


Fig. 5. Dependence of  $\omega$  XRD 0002 peak FWHM for a wurtzite  $\text{Al}_x\text{Ga}_{1-x}\text{N}$  layers ( $x \sim 0.2$ ) on the growth time.

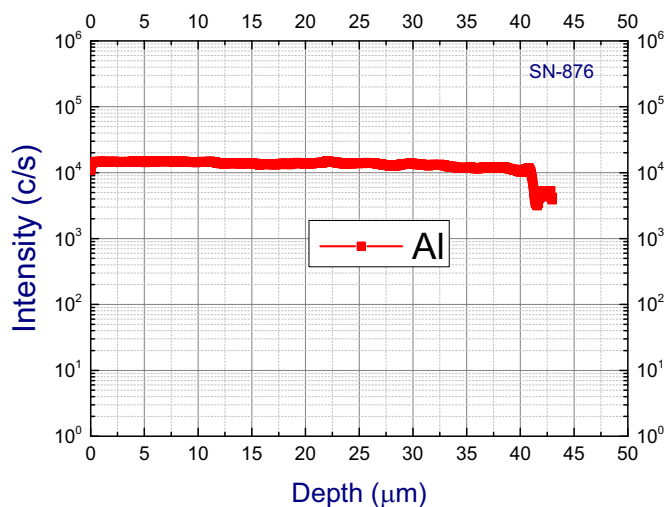


Fig. 6. SIMS profiles for Al for a w- $\text{Al}_x\text{Ga}_{1-x}\text{N}$  layer ( $x \sim 0.2$ ).

$\text{Ga}_{1-x}\text{N}$  film. In XRD studies we observed a single 0002 peak at  $\sim 35^\circ$ , consistent with a wurtzite  $\text{Al}_x\text{Ga}_{1-x}\text{N}$  layer. For  $\text{Al}_x\text{Ga}_{1-x}\text{N}$  layers with increasing Al content we observed a gradual shift of the position of the 0002  $\text{Al}_x\text{Ga}_{1-x}\text{N}$  peak in  $2\theta$ - $\omega$  XRD plots to higher angles as expected. Using Vegard's Law, we can estimate the composition of the  $\text{Al}_x\text{Ga}_{1-x}\text{N}$  layer shown in Fig. 4 to be  $x \sim 0.2$ . The AlN fraction in this  $\text{Al}_x\text{Ga}_{1-x}\text{N}$  layer was also confirmed by both SIMS and EDX measurements. From high resolution XRD scans we can estimate the zinc-blende fraction, which in this case was below our detection limit ( $< 0.1\%$ ).

Fig. 5 shows the full-width-at-half-maximum (FWHM) of the 0002 peak at  $\sim 35^\circ$  from XRD  $\omega$ -plots for several wurtzite  $\text{Al}_x\text{Ga}_{1-x}\text{N}$  layers grown on 3-inch GaAs as a function of growth time. The  $\text{Al}_x\text{Ga}_{1-x}\text{N}$  layers were grown at a growth rate of  $\sim 2.2 \mu\text{m/h}$  and with an AlN content of  $x \sim 0.2$ . The growth time was up to 50 h and the thickness of the layers was up to  $\sim 100 \mu\text{m}$ . In all of our earlier experiments with the growth of bulk zinc-blende  $\text{Al}_x\text{Ga}_{1-x}\text{N}$  layers, we observed degradation of the crystal quality of the layers with increasing thickness due to a gradual build-up of the concentration of wurtzite inclusions in the zinc-blende matrix. In the current research, the structural quality of the wurtzite  $\text{Al}_x\text{Ga}_{1-x}\text{N}$  layer improves rapidly with increasing layer thickness

during the first few hours of growth. This is due to cubic inclusions close to the GaN/GaAs interface reverting to wurtzite after approximately 70 nm of growth. There is also a steady reduction in the density of stacking faults in the film, which are readily generated by growth on mixed phase material close to the GaN/GaAs interface. However, we are still investigating the mechanisms behind that. The structural quality of  $\text{Al}_x\text{Ga}_{1-x}\text{N}$  then slightly degrades during further MBE growth. This may arise because we are probably shifting from the optimum growth temperature and Ga/N flux ratio after the first ten hours of growth, due to depletion of Ga in the Ga SUMO-cell during the long growths with high fluxes of BEP  $\sim 2 \times 10^{-6}$  Torr.

The depth uniformity of Al incorporation in the  $\text{Al}_x\text{Ga}_{1-x}\text{N}$  layers was studied using SIMS. As SIMS studies show the Al, Ga and N profiles are uniform with depth. Fig. 6 demonstrates Al distribution only in a  $\sim 42 \mu\text{m}$ -thick AlGaN layer with an AlN of  $\sim 20\%$ . The profile is from the center of the film and there may be small variations in Al:Ga ratio as a function of radial position. There was no significant As incorporation into the bulk of thick AlGaN layers and the detected As was at the background level of the SIMS system, as have been demonstrated previously [8,10].

#### 4. Summary and conclusions

We have grown free-standing  $\text{Al}_x\text{Ga}_{1-x}\text{N}$  layers with thicknesses up to  $100 \mu\text{m}$  by PA-MBE using the latest Riber model of fast-growth Riber RF plasma source. We have demonstrated that AlGaN layers grown on GaAs (111)B substrates have N-polarity. Free-standing bulk  $\text{Al}_x\text{Ga}_{1-x}\text{N}$  wafers with thicknesses in the 30–100  $\mu\text{m}$  range may be used as substrates for further growth of  $\text{Al}_x\text{Ga}_{1-x}\text{N}$ -based structures and devices. The novel high efficiency RF plasma source allowed us to achieve such  $\text{Al}_x\text{Ga}_{1-x}\text{N}$  thicknesses on 3-inch diameter wafers in a single day's growth, which makes our bulk growth technique potentially commercially viable.

#### Acknowledgments

This work was undertaken with support from the EPSRC (EP/K008323/1). We want to acknowledge Loughborough Surface Analysis Ltd for SIMS measurements and discussions of results.

#### References

- [1] J.H. Edgar, S. Strite, I. Akasaki, H. Amano, C. Wetzel (Eds.), Gallium Nitride and Related Semiconductors, INSPEC, Stevenage, 1999, ISBN 0 85296 953 8.
- [2] M. Shatalov, W. Sun, A. Lunev, X. Hu, A. Dobrinsky, Y. Bilenko, J. Yang, M. Shur, R. Gaska, C. Moe, G. Garrett, M. Wraback, Appl. Phys. Express 5 (2012) 082101.
- [3] H. Hirayama, N. Noguchi, T. Yatabe, N. Kamata, Appl. Phys. Express 1 (2008) 051101.
- [4] Z. Ren, Q. Sun, S.-Y. Kwon, J. Hana, K. Davitt, Y.K. Song, A.V. Nurmikko, H.-K. Cho, W. Liu, J.A. Smart, L.J. Schowalter, Appl. Phys. Lett. 91 (2007) 051116.
- [5] Z. Bryan, I. Bryan, S. Mita, J. Tweedie, Z. Sitar, R. Collazo, Appl. Phys. Lett. 106 (2015) 232101.
- [6] A. Belousov, S. Katrych, J. Jun, J. Zhang, D. Gunther, R. Sobolewski, J. Karpinski, B. Batlogg, J. Cryst. Growth 311 (2009) 3971.
- [7] Y.V. Melnik, V.A. Soukhoveev, K.V. Tsvetkov, V.A. Dmitriev, MRS Symp. Proc. 764 (2003) 363.
- [8] S.V. Novikov, C.R. Staddon, R.E.L. Powell, A.V. Akimov, F. Luckert, P.R. Edwards, R.W. Martin, A.J. Kent, C.T. Foxon, J. Cryst. Growth 322 (2011) 23.
- [9] B.M. McSkimming, F. Wua, T. Huault, C. Chaix, J.S. Speck, J. Cryst. Growth 386 (2014) 168.
- [10] S.V. Novikov, C.R. Staddon, R.W. Martin, A.J. Kent, C.T. Foxon, J. Cryst. Growth 425 (2015) 125.
- [11] B.M. McSkimming, C. Chaix, J.S. Speck, J. Vac. Sci. Technol. A 33 (2015) 05E128.
- [12] O. Takahashi, T. Nakayama, R. Souda, F. Hasegawa, Phys. Status Solidi b 228 (2001) 529.